NASA/TM—2000-210471/REV1

Micromechanical and Electrical Properties of Monolithic Aluminum Nitride at High Temperatures

Jon C. Goldsby
Glenn Research Center, Cleveland, Ohio

January 2001

The NASA STI Program Office . . . in Profile

Since its founding, NASA has been dedicated to the advancement of aeronautics and space science. The NASA Scientific and Technical Information (STI) Program Office plays a key part in helping NASA maintain this important role.

The NASA STI Program Office is operated by Langley Research Center, the Lead Center for NASA's scientific and technical information. The NASA STI Program Office provides access to the NASA STI Database, the largest collection of aeronautical and space science STI in the world. The Program Office is also NASA's institutional mechanism for disseminating the results of its research and development activities. These results are published by NASA in the NASA STI Report Series, which includes the following report types:

- TECHNICAL PUBLICATION. Reports of completed research or a major significant phase of research that present the results of NASA programs and include extensive data or theoretical analysis. Includes compilations of significant scientific and technical data and information deemed to be of continuing reference value. NASA's counterpart of peer-reviewed formal professional papers but has less stringent limitations on manuscript length and extent of graphic presentations.

- TECHNICAL MEMORANDUM. Scientific and technical findings that are preliminary or of specialized interest, e.g., quick release reports, working papers, and bibliographies that contain minimal annotation. Does not contain extensive analysis.

- CONTRACTOR REPORT. Scientific and technical findings by NASA-sponsored contractors and grantees.

- CONFERENCE PUBLICATION. Collected papers from scientific and technical conferences, symposia, seminars, or other meetings sponsored or cosponsored by NASA.

- SPECIAL PUBLICATION. Scientific, technical, or historical information from NASA programs, projects, and missions, often concerned with subjects having substantial public interest.

- TECHNICAL TRANSLATION. English-language translations of foreign scientific and technical material pertinent to NASA's mission.

Specialized services that complement the STI Program Office's diverse offerings include creating custom thesauri, building customized data bases, organizing and publishing research results . . . even providing videos.

For more information about the NASA STI Program Office, see the following:

- Access the NASA STI Program Home Page at ***http://www.sti.nasa.gov***

- E-mail your question via the Internet to help@sti.nasa.gov

- Fax your question to the NASA Access Help Desk at 301–621–0134

- Telephone the NASA Access Help Desk at 301–621–0390

- Write to:
  NASA Access Help Desk
  NASA Center for AeroSpace Information
  7121 Standard Drive
  Hanover, MD 21076

NASA/TM—2000-210471/REV1

Micromechanical and Electrical Properties of Monolithic Aluminum Nitride at High Temperatures

Jon C. Goldsby
Glenn Research Center, Cleveland, Ohio

National Aeronautics and
Space Administration

Glenn Research Center

January 2001

Acknowledgments

Thanks to Dr. Paul Angel and Mr. Douglass Doza for the dielectric property measurements.

Available from

NASA Center for Aerospace Information
7121 Standard Drive
Hanover, MD 21076
Price Code: A03

National Technical Information Service
5285 Port Royal Road
Springfield, VA 22100
Price Code: A03

Available electronically at http://gltrs.grc.nasa.gov/GLTRS

MICRO-MECHANICAL AND ELECRICAL PROPERTIES OF MONOLITHIC ALUMINUM NITRIDE AT HIGH TEMPERATURES

Jon C. Goldsby
National Aeronautics and Space Administration
Glenn Research Center
Cleveland, Ohio 44135

SUMMARY

Micromechanical spectroscopy of aluminum nitride reveals it to possess extremely low background internal friction at less than 1×10^{-4} logarithmic decrement (log dec.) from 20 to 1200 °C. Two mechanical loss peaks were observed, the first at 350 °C approximating a single Debye peak with a peak height of 60×10^{-4} log dec. The second peak was seen at 950 °C with a peak height of 20×10^{-4} log dec. and extended from 200 to over 1200 °C. These micromechanical observations manifested themselves in the electrical behavior of these materials. Electrical conduction processes were predominately intrinsic. Both mechanical and electrical relaxations appear to be thermally activated processes, with activation energies of 0.78 and 1.32 eV respectively.

INTRODUCTION

Aluminum nitride has been shown to have great potential as a high temperature electronic packaging material (refs. 1 to 3). However in extreme environment applications, low amplitude ($<10^{-6}$ strain) vibrations can be a source of mechanical fatigue and failure. In addition, elevated temperatures encountered during device fabrication and during subsequent operation demand knowledge of the material's temperature dependent mechanical and electrical response. To obtain this information, resonance frequency and internal friction measurements were performed on aluminum nitride as a function of temperature. The temperature and frequency dependent dielectric properties were also measured and compared with the micro-mechanical measurements to elucidate a probable mechanism for the observed behavior.

EXPERIMENTAL

Samples of a commercially available aluminum nitride (density 3.27 g/cm^3), with small additions of Y_2O_3 (~1 wt.%) as a consolidation aid, were sectioned into specimens with dimensions 114×9×3 mm. Temperature dependent elastic and anelastic properties were determined by establishing continuous flexural vibrations in the specimen at its lowest resonance frequency and allowing the vibrations to freely decay after the mechanical excitation was removed. The details of the apparatus are given elsewhere (4). At a constant frequency (f) the unit for anelastic behavior is the logarithmic decrement ψ and it is calculated as,

$$\psi = \frac{\ln\left(a_1/a_2\right)}{(f)(t_2 - t_1)} \tag{1}$$

where amplitudes a_1 and a_2 are measured at times t_1 and t_2, respectively (11). The geometry and material dependent resonance frequency can be calculated from,

$$f = \left(\frac{B}{l^2}\right)\left(\frac{E}{\rho}\right)^{\frac{1}{2}} \tag{2}$$

where B is a combination of geometric and numeric constants, l is the sample length, and E and ρ are the material's elastic modulus and density, respectively. From equation (2), a ratio of the resonance frequencies, at a given temperature with respect to the 25 °C value, gives a measure of the temperature dependent elastic response. To obtain the electrical measurements, specimens of aluminum nitride were plated with platinum electrodes. The electric permittivity as a function of temperature and frequency was measured in air using a Solatron 1260 impedance analyzer as previously reported (5). Micrographs of etched and polished samples were recording using scanning electron microscopy. Energy dispersion spectroscopy EDS was used to identify the various major phases of this material.

RESULTS AND DISCUSSION

A typical SEM micrograph is seen in figure 1, where three types of features with various amounts of yttrium, alumina, and carbon are clearly revealed. The observed carbon may be only an artifact from the microscope probe analysis. Micrographs of a cut and polished surface reveal grains free of excessive boundary phases. X-ray diffraction also indicates a highly crystalline material. Yttrium-containing compounds appear at grain boundary triple points. In addition, EDS reveals the presence of alumina among the AlN grains.

The mechanical spectrum in figure 2 illustrates the anelastic and elastic responses of this material up to 1200 °C, at a fundamental vibration of 1464 Hz. This mechanical loss spectrum contains two peaks. The salient features of the first peak include its location at 350 °C, with a peak height of 60×10^{-4} log dec. The peak commences at about 200 °C and terminates at approximately 500 °C. This energy loss peak closely approximates a Debye peak with a narrow distribution of thermally activated relaxation times. The second mechanical energy loss peak was observed at 950 °C, and is designated the high temperature peak. The high temperature peak is a low amplitude, broad peak starting at approximately 200 °C and extending beyond 1200 °C. In addition, the mechanical loss spectrum was also obtained at the first overtone to the fundamental frequency, which for this material, vibration mode and geometry was 4087 Hz. This spectrum exhibits the same features as the fundamental tone with the exception of the first overtone peak, which is spectrum-shifted to the right with respect to the temperature. This thermal and mechanical coupling indicates a thermally activated mechanism as the source of the elastic and anelastic dispersion. Noticeably absent is the exponential increase in background internal friction characteristic of the grain boundary sliding observed in silicon nitride (6). In addition, figure 2 also illustrates a decrease or relaxation in the elastic modulus, which occurs at the same temperature as the anelastic relaxation absorption peak at 350 °C. The typical elastic response as a function of temperature is shown in the upper curve in figure 2. This figure illustrates that the relative stiffness of the material decreases 8 percent from 25 to 1200 °C, which is not unusual for monolithic ceramic materials (4). In addition features of the elastic response, illustrated in figure 2, also shifts to higher temperatures when the sample is mechanical excited at its first overtone. This behavior is indicative of thermally activated mechanism. Because such a low level of internal friction exist around the peaks and the corresponding temperature dependent elasticity remains relatively constant, no evidence of grain boundary sliding induced micro-creep is evident, under the conditions of the micro-strains imposed on the aluminum nitride samples in this investigation.

Given the reported piezoelectric nature of bulk and thin film AlN (7), temperature dependent dielectric measurements were performed to determine if these micromechanical observations manifested themselves in the electrical properties of this material. The complex electric modulus (M) formalism was used to characterize the material's temperature dependent dielectric properties (refs. 8 and 9). The complex electric modulus is the reciprocal of the complex permittivity ε. The relationship between the permittivity and the electric modulus is given in equation (3)

$$M = \frac{1}{\varepsilon} = \frac{\varepsilon_{\text{Real}}}{\varepsilon^2_{\text{Real}} + \varepsilon^2_{\text{Imaginary}}} + j\frac{\varepsilon_{\text{Imaginary}}}{\varepsilon^2_{\text{Real}} + \varepsilon^2_{\text{Imaginary}}} \tag{3}$$

The complex electric modulus plot gives a single arc, which is representative of the bulk properties of the material (fig. 3). From this data, the magnitude of the imposed alternating electric field and sample dimensions, the direct current resistivity was determined to be 10^8 Ω/meters. Therefore this AlN sample, with predominately covalent bonding, behaves like an insulator and hence contains minimal concentrations of those agents, which could function as extrinsic charge carrying dopants.

Results shown in figure 4 illustrate a dispersion of the real part of the electric modulus. The midpoints of these dispersion curves occur at 10, 20, 30, and 70 kHz for these temperatures 466, 490, 515, and 550 °C respectively. The peaks in figures 5(a) and 5(b) appear thermally activated and are located near the temperature of the mechanical internal friction peak found at 400 °C and 4087 Hz. Each peak extends over three decades of frequency, indicating a wide range of relaxation times due to the non-degenerate reorientation of elastic strain energy states of the relaxing entities. At higher temperatures (560 to 734°C), the complex component of the electric modulus becomes narrower and higher as compared to the lower temperature results (figs. 5(a) and 5(b)). In addition it is at these temperatures that the two mechanical loss peaks overlap in figure 2. The smaller peak at 560 °C in figure 5(b) appears to be a continuation of the low temperature peaks seen in figure 5(a). The higher and narrower absorption curves in figure 5(b), suggest a different source of origin, possibly one that is related to the high temperature loss peak in figure 2.

Both the mechanical and electrical energy absorption peaks can be treated as thermally activated Arrhenius processes to obtain their respective activation energies. The energy equation is classically expressed as

$$f(T) = f_o e^{(-Q/kT)} \tag{4}$$

were f(T) is the temperature dependent resonance frequency, f_o is the characteristic frequency of the relaxation phenomenon, k and T are the Boltzmann constant and absolute temperature, respectively, and Q represents the activation energy. A plot of the peak frequency as a function of reciprocal temperature is given in figure 6. From the slope of these lines the activation energy was found to be 0.78 eV for the T= 350 °C mechanical anelastic peak. Activation energies derived from the electric modulus were 1.32 and 1.18 eV for the low temperature and high temperature peaks, respectively. Nakayama et al. (10) have observed the loss tangent as a function of grain size, and attributed the energy absorption peak to the piezoelectric effect in AlN crystal grains at 830 MHz and 30 °C. Hence in this study the magnitude of the thermal activation energies, temperatures, frequencies and height of the mechanical absorption peak indicate that the piezoelectric effect is not the source of the observed mechanical or electrical dispersion in the loss factors. The results of this investigation are more indicative of point defects or a cluster of point defects as the likely cause of the electrical and mechanical relaxation (refs. 10 and 11).

Slack et al. (12) have identified oxygen as a major impurity in aluminum nitride. One possible source of oxygen clearly would be the consolidation additives, examples of which are Al_2O_3 and Y_2O_3 as seen in figure 1. Equation (5) is the proposed mechanism for the incorporation of M_2O_3, where M is a metal in the (+3) state, into AlN expressed in Kroger-Vink notation. In this scenario lattice misfit strain occurs due to the smaller ionic radii of the incorporated oxygen, as compared with the nitrogen ion of the host crystal. In addition, to compensate for the difference in valance, charged (+2) vacancies on the aluminum sites are created.

$$M_2O_3 \overset{AlN}{\leftrightarrow} 2M_{Al}^{*} + 3O_N^{*} + V_{Al}^{'''} \tag{5}$$

The resultant physical entity, which is described by equation (5), is a charged defect cluster within the AlN crystal lattice. This defect or electro-elastic dipole would respond to both external mechanical and electrical alternating fields. The probable cause for the different magnitudes between the mechanical and electrical activation energies at the lower temperatures may be due to the difference in the elastic strain energy barrier to reorientation. The externally applied alternating mechanical stress field may provide sufficient elastic strain energy to reduce the reorientation barrier and hence lower the activation energy needed for the defect's reorientation. A similar effect may be functioning at the higher temperature electric relaxation. At higher temperatures a more isotropic stress state may exist due to thermal expansion of the crystal lattice and thereby lowering the activation energy for defect reorientation.

CONCLUSIONS

Temperature dependent elastic, anelastic, and electrical properties of AlN were characterized by micro-mechanical and dielectric measurements. Intrinsic damping in aluminum nitride was below that needed to suppress vibrations at temperatures below 1200 °C in vacuum. In addition, alternating stress and electrical fields induced dipole reorientation of vacancy defects. The elastic modulus only decreased by 8 percent under the conditions of this investigation (20 to 1200 °C), and hence aluminum nitride has potential of retaining stiffness and dimensional tolerances at elevated temperatures.

REFERENCES

1. A.F. Belyanin, L.L. Bouilov, V.V. Zhirnov, A.I. Kamenev, K.A. Kovalskij and B.V. Spitsyn, "Application of aluminum nitride films for electronic devices," Diamond and Related Materials, vol. 8, nos. 2–5, pp. 369–372, 1999.
2. S.P. McGeoch, F. Placido, Z. Gou, C.J.H. Wort, and J.A. Savage, "Coatings for the protection of diamond in high-temperature environments," Diamond and Related Materials, vol. 8, nos. 2–5, pp. 916–919, 1999.
3. J.H. Harris, "Sintered aluminum nitride ceramics for high-power electronic applications," JOM, vol. 50, no. 6, pp. 56–60, 1998.
4. J.C. Goldsby, "Temperature-dependent elastic and anelastic behavior of silicon-based fiber reinforced silicon carbide ceramic matrix composites." Materials Science and Engineering A, vol. A279, pp. 266–74, 2000.
5. P.W. Angel, M.R. De Guire, and A.R. Cooper, " Electrical conductivity, relaxation and the glass transition: A new look at a familiar phenomenon," Journal of Non-Crystalline Solids, vol. 203, pp. 286–292, 1996.
6. R. Raj, and M.F. Ashby, "On Grain Boundary Sliding and Diffusion Creep," Metallurgical Transactions, vol. 2, pp. 1113–1127, (1971).
7. A. Nakayanna, S. Nambu, M. Inagaki, M. Miyauchi, and N. Itoh "Dielectric Dispersion of Polycrystalline Aluminum nitride at microwave frequencies." Journal of the American Ceramic Society, Iss 6, vol. 79, pp. 1453–56, 1996.
8. I.M. Hodge, M.D. Ingram, and A.R. West, "Impedance and modulus spectroscopy of polycrystalline solid electrolytes." Journal of Electroanalytical Chemistry and Interfacial Electrochemistry. Vol. 74, pp. 125–43, 1976.
9. I.M. Hodge, M.D. Ingram, and A.R. West, "A new method for analyzing the a. c. behaviour of polycrystalline electrolytes." Electroanalytical Chemistry and Interfacial Electrochemistry. Vol. 58, pp. 429–32, 1975.
10. L. Murawski, R.J. Barczynski, D. Samatowicz, and O. Gzowski, " Correlation between mechanical and electrical losses in transition metal oxide glasses." Journal of Alloys and Compounds. Vol. 211/212, pp. 344–48. 1994.
11. A.S. Nowick and B.S. Berry, Anelastic Relaxation in Crystalline Solids, Academic Press New York and London (1972).
12. G.A. Slack, R.A. Tanzilli, R.O. Pohl, and J.W. Vandersande, "The intrinsic thermal conductivity of AlN." Journal of physics and Chemistry of Solids. Vol. 48, no. 78, pp. 641–47, 1987.

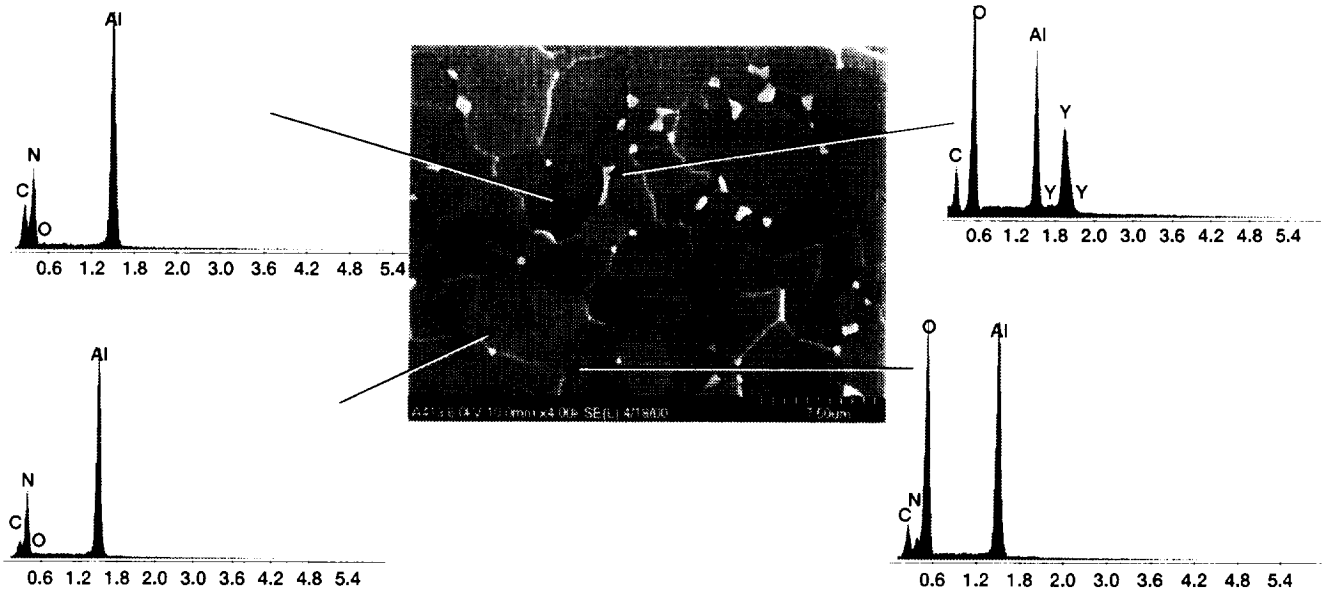

Figure 1.—Secondary electron image of aluminum nitride sample with EDS results illustrating composition.

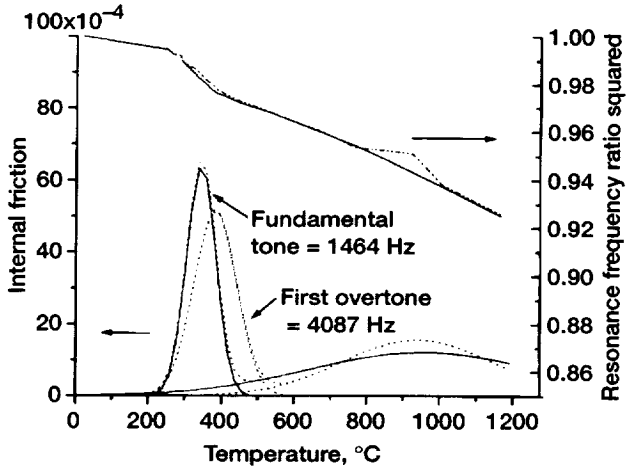

Figure 2.—Temperature dependent elastic and anelastic behavior of aluminum nitride at the fundamental and first overtone flexural vibration frequencies.

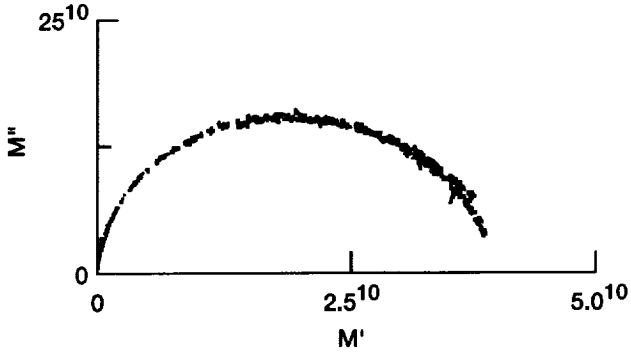

Figure 3.—Complex electric modulus plot of aluminum nitride.

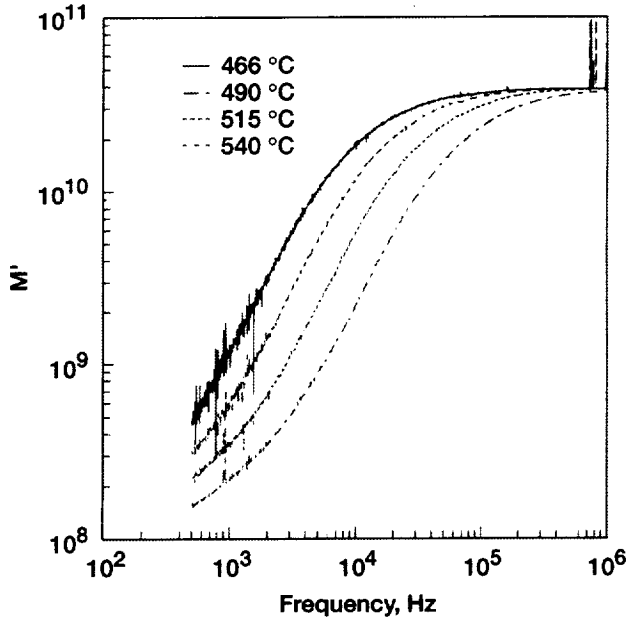

Figure 4.—Frequency and temperature dependent real part of the electric modulus.

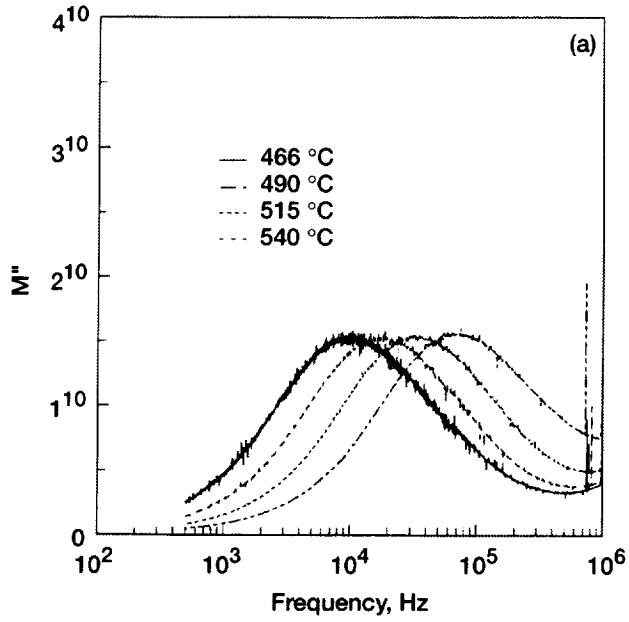

Figure 5.—Frequency and temperature dependence of the imaginary part of the electric modulus (a) from 466 °C to 540 °C and (b) from 560 °C to 638 °C.

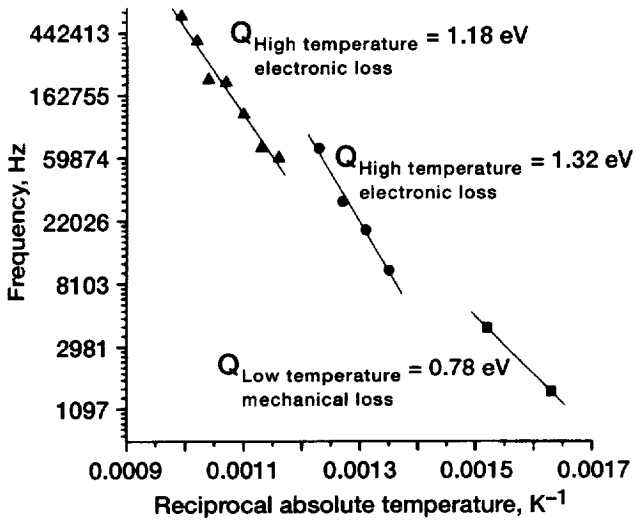

Figure 6.—Determination of activation energies for mechanical and electronic loss processes in aluminum nitride.

REPORT DOCUMENTATION PAGE

Form Approved
OMB No. 0704-0188

1. AGENCY USE ONLY (*Leave blank*)	2. REPORT DATE	3. REPORT TYPE AND DATES COVERED
	January 2001	Technical Memorandum

4. TITLE AND SUBTITLE

Micromechanical and Electrical Properties of Monolithic Aluminum Nitride at High Temperatures

5. FUNDING NUMBERS

WU–523–31–13–00

6. AUTHOR(S)

Jon C. Goldsby

7. PERFORMING ORGANIZATION NAME(S) AND ADDRESS(ES)

National Aeronautics and Space Administration
John H. Glenn Research Center at Lewis Field
Cleveland, Ohio 44135–3191

8. PERFORMING ORGANIZATION REPORT NUMBER

E–12439–1

9. SPONSORING/MONITORING AGENCY NAME(S) AND ADDRESS(ES)

National Aeronautics and Space Administration
Washington, DC 20546–0001

10. SPONSORING/MONITORING AGENCY REPORT NUMBER

NASA TM—2000-210471-REV1

11. SUPPLEMENTARY NOTES

Responsible person, Jon C. Goldsby, organization code 5130, 216–433–8250.

12a. DISTRIBUTION/AVAILABILITY STATEMENT

Unclassified - Unlimited
Subject Categories: 27 and 76 Distribution: Nonstandard

Available electronically at http://gltrs.grc.nasa.gov/GLTRS
This publication is available from the NASA Center for AeroSpace Information, 301–621–0390.

12b. DISTRIBUTION CODE

13. ABSTRACT ***(Maximum 200 words)***

Micromechanical spectroscopy of aluminum nitride reveals it to possess extremely low background internal friction at less than 1×10^{-4} logarithmic decrement (log dec.) from 20 to 1200 °C. Two mechanical loss peaks were observed, the first at 350 °C approximating a single Debye peak with a peak height of 60×10^{-4} log dec. The second peak was seen at 950 °C with a peak height of 20×10^{-4} log dec. and extended from 200 to over 1200 °C. These micromechanical observations manifested themselves in the electrical behavior of these materials. Electrical conduction processes were predominately intrinsic. Both mechanical and electrical relaxations appear to be thermally activated processes, with activation energies of 0.78 and 1.32 eV respectively.

14. SUBJECT TERMS	15. NUMBER OF PAGES
Electronic materials; Aluminum nitride high temperature properties; Internal friction high temperature dielectric measurements; Functional ceramics high temperatures	14
	16. PRICE CODE: A03

17. SECURITY CLASSIFICATION OF REPORT	18. SECURITY CLASSIFICATION OF THIS PAGE	19. SECURITY CLASSIFICATION OF ABSTRACT	20. LIMITATION OF ABSTRACT
Unclassified	Unclassified	Unclassified	